Giant, 18, 2024, 100253

Full-length article

Facile fabrication of high-strength biocomposite through Mg^{2+}-enhanced bonding in bamboo fiber

Shengbo Ge[a], Guiyang Zheng[a], Yang Shi[a], Zhongfeng Zhang[b,*], Abdullatif Jazzar[c], Ximin He[c,*], Saddick Donkor[d], Zhanhu Guo[d], Ding Wang[d], Ben Bin Xu[d,*]

[a] Co-Innovation Center of Efficient Processing and Utilization of Forest Resources, College of Materials Science and Engineering, Nanjing Forestry University, Nanjing 210037, China
[b] College of Furniture and Art Design, Central South University of Forestry and Technology, Changsha, Hunan 410004, China
[c] Department of Materials Science and Engineering, University of California, Los Angeles (UCLA), Los Angeles, CA 90095, USA
[d] Department of Mechanical and Construction Engineering, Northumbria University, Newcastle Upon Tyne, NE1 8ST, UK

Keywords: Bamboo, Biocomposite, Metal ion coordination, Environmental sustainability

The emerging interests in high-performance biocomposites grows significantly driven by their superior environmental sustainability. This study proposes a unique biocomposite strategy by implementing an acetic and ball-milled treatment to disrupt the bamboo cell wall structure, thereby facilitating further processing by effectively increasing the active sites and specific surface area in the bamboo fiber. The fibers are subsequently carboxymethylated to introduce carboxyl groups which facilitate physical bonding between the fibers and Mg^{2+} ions that are added to the system. These ions form metal-coordination bonds with the carboxyl groups, acting as ion bridges that significantly strengthen the inter-fiber bonding. The resulted biocomposite exhibits impressive mechanical properties, including a high tensile strength (94.24 MPa) and flexural strength (104.14 MPa), not only that, changes in elastic modulus also highlight changes in fiber bonding, the flexural modulus is 21.29 GPa and the tensile modulus is 7.01 GPa. Moreover, it maintains a low water uptake capacity of only 6.8 % despite being submerged for 12 h. The thermal conductivity and fire retardancy have also been improved. The synergic bonding ability between the cellulose and lignin in the fibers, coupled with the glue-free thermoforming process, enhances the material performance and renders it fully recyclable, thus reducing environmental pollution and providing cost-effective engineering materials to society.

Introduction

Since ancient times, humans have used natural biomass for various purposes, such as fuel and construction materials [1–2]. As industrial development advanced, low-cost yet high-performance materials became more prevalent in construction [3–5]. However, while these materials have proven useful, their widespread use has resulted in significant amounts of non-degradable waste, leading to concerns related to human health and the environment [6–8]. Moreover, the manufacturing of these materials generates various harmful by-products, including acid wastewater, heavy metals, VOCs (volatile organic compounds) and respirable particulate

* Corresponding authors.
E-mail addresses: csfuzzf@163.com (Z. Zhang), ximinhe@ucla.edu (X. He), ben.xu@northumbria.ac.uk (B.B. Xu).
Received 28 December 2023; Received in revised form 11 February 2024; Accepted 14 March 2024

 https://doi.org/10.1016/j.giant.2024.100253

matter, and greenhouse gases that contribute to water and air pollution [9–11].

As the world faces unprecedent environmental challenges, researchers are exploring innovative ways to mitigate the negative impacts caused by the processing of biomass [12–13]. Efficient modification strategies can significantly enhance the subpar performance of natural biomass, specifically its durability and mechanical strength [14]. These modifications can facilitate the advancement and application of eco-friendly materials, thereby contributing significantly to environmental conservation efforts [15–17]. Among various biomass, bamboo stands out due to its fast growth rate, short growth cycle, as well as its simple and straight structure, making it an ideal candidate for biocomposite production [18–21]. However, the limited diameter of bamboo poses challenges in producing large-size veneers using traditional slicing or rotary cutting methods, thus disadvantage it's further application [22]. Recently, the use of broken bamboo as a precursor for fiberboard or particleboard production shows great potential for scale-up fabrication [23–26].

Biomass engineering materials are also hindered by weak mechanical properties and poor durability [27–28]. A conventional approach to reinforce bamboo is to fill bamboo fiber gaps with adhesives [28–30]. However, the use of such adhesives can result in formaldehyde emission that poses a health hazard to humans. Additionally, the performance of glue-free bamboo fiberboard is impractical for biocomposite applications [31–33]. The most common reinforcing technique to achieve ideal mechanical properties and durability, is to add plastic to make plastic/bamboo hybrid. Such approach draw considerable concerns on the subsequent waste, which bring more challenges on the circular economy remits [34–35].

Various pretreatment methods are helpful to improve the performance of glue-free bamboo fiber boards [33]. Treatment with acidic and alkaline solutions has shown advantage in enhancing mechanical properties [36]. A variety of salt solutions can also be used for fiber treatment, which not only provide suitable pH for pretreatment, but also introduce ions so that they can participate in fiber bonding and enhance their performance [37].

Herein, we introduce a novel fabrication strategy to achieve high performance bamboo-based biocomposites. Our method employs a combination of acid etching and carboxymethylation to modify bamboo fiberboards. The removal of hemicellulose, inclusion of carboxyl groups, and the addition of Mg^{2+} to facilitate fiber bonding through metal-coordination bonds formation during hot pressing not only significantly enhances the mechanical properties and durability of the board, but also offers an environmentally friendly process by eliminating pollutant emission. The complete glue-free strategy used in this modification also enhances the recyclability of the board, thereby reducing environmental pollution and resource wastage.

Materials and methods

Materials

Phyllostachys heterocycle (meso bamboo) was purchased from Shenglong bamboo and woodcraft products factory. To ensure that the experiment utilised the highest quality raw material, the bamboo powder was meticulously screened, with only the 60–100 mesh of bamboo powder being deemed suitable for further use, placed the bamboo powder in an oven at 60 °C until the quality did not change. Acetic acid (purity: 99.5 %), sodium hydroxide (purity: 96 %) and magnesium chloride (purity: 99.5 %) were purchased from Sinopharm Chemical Reagent Co., Ltd. Sodium chloroacetate (purity: 98 %) was purchased from Aladdin Biochemical Technology Co., Ltd in Shanghai.

Preparation of acid-etched bamboo powder

To prepare the acid-etched bamboo powder, we began by mixing bamboo powder with 9 wt% aqueous acetic acid in a ratio of 1 g of powder to 6 mL acid. The mixture was then subsequently inserted into a metallic ball mill cup, which was equipped with 6 balls of 8.1 mm diameter and another 6 balls of 4.25 mm diameter. The cup was securely fastened into a BP-R8 multi-vessel rotary mixer manufactured by Hefei Kejing Material Technology Co., Ltd. The mixing process was conducted at a temperature of 150 °C and a stirring speed of 300 rpm for a total duration of 4 h. Once the temperature returned to the ambient level, the cup was removed from the mixer and carefully washed with deionised water. This step was crucial to neutralize any remaining acidic content. Subsequently, the acid-etched bamboo powder was successfully prepared, ready for further applications.

Preparation of enhanced bamboo powder

In the carboxymethylation of the treated bamboo powder, a mixture consisting of 20 g of acid-etched bamboo powder, 6.6 g of sodium chloroacetate, and 240 mL of distilled water was heated for four hours at 60 °C in a water bath. Subsequently, 3 wt% aqueous sodium hydroxide was added to the mixture, which was then further heated for 70 min at 75 °C. The resulting dried powder is named carboxymethylated powder. The carboxymethylated powder was repeatedly washed with absolute ethanol and subsequently dried in an oven. To enhance this powder further, 10 g of carboxymethylated powder, 140 g of a 30 wt% magnesium chloride solution (30 wt%), and 280 mL of ethanol was mixed. This mixture was then heated ed in a 70 °C water bath for 180 min. The by-product of the reaction was rinsed out with deionised water, yielding the enhanced powder.

Preparation of enhanced biocomposites

The production of reinforced biocomposites commenced with the desiccation of bamboo powder in an oven at 60 °C for 24 h. Subsequently, the sample was exposed to stable relative ambient temperature and humidity to balance the moisture content. The dried bamboo powder was then subjected to hot pressing, applying a 90 min heating at 185 °C and pressure of 30 MPa. Once the hot-pressing process was completed, the obtained specimen was left to naturally chill to the surrounding temperature (Fig. 1). For the control group, untreated bamboo powder underwent the same processing steps as the reinforced biocomposites.

Measurements of physical properties of reinforced bamboo composites

Conforming to the GB/T 17657-2013 standards, the composite materials were subjected to comprehensive testing to evaluate

Fig. 1

A schematic figure detailing the steps to produce the enhanced biocomposite.

their density, mechanical strength (including tensile and bending strengths), and water absorption characteristics [38]. Each sample was subjected to three rounds of testing, with the mean value used for analysis. The mechanical strength (bending and tensile) of the composite materials was evaluated by adopting the Shimadzu AGS-X universal testing machine (Japan). The testing parameters included a sample size of 50 × 7 × 2.2 mm, a crosshead speed of 0.2 cm/min, and a distance of 1.7 cm among the lower and upper ends. Additionally, the bending strength was measured using a three-point bending machine at a span of 3 cm and a crosshead acceleration of 1 cm/min. To gauge water resistance, the samples were immersed in water and monitored for changes in thickness and water content at intervals of 3, 6, 9, 12, 24, and 48 h.

A contact angle tester (DSA100S, KRUSS) was employed to determine the surface wettability. The degree of contact angle was quantified by capturing photographs of the shape and contact angle of water droplets on the sample surface. A 10 mg powder sample was placed in a TGA55 thermogravimetric analyser (TA Instruments). The temperature was raised from room temperature to 750 °C at a heating rate of 10 °C/min. Under different magnifications and acceleration voltage of 15 kV, the microscopic morphology of sample surface and cross-section was scanned and analysed with an electronic fiber microscope. The thermal conductivity of sample (20 × 20 × 2.5 mm) was measured with a DRPL-2B thermal constant analyser. The test of specific surface area is provided by Bester specific surface area and pore analyzer, and the degassing temperature is 110 °C for 12 h.

Quantification of the properties and chemical content of reinforced bamboo composites

To determine the lignin composition that is insoluble in acid, the following procedure [39] is performed. Approximately 30 mg of the powdered specimen was introduced to a borosilicate container containing 3 mL sulfuric acid (72 %). The container was then sealed and placed in a water bath at 30 °C for an hour. Then, deionised water (about 84 mL) was used to top-up into the container before it was sealed, after which the container was subjected to high-temperature sterilisation for 60 min prior to solid-liquid separation. Resulting solid components were washed, neutralised by deionised water, and then dried before being incinerated at 540 °C for 6 h in a high-temperature furnace (KSL-1200X-J) manufactured by Hefei Kejing Material Technology Co., Ltd. in China.

A P4PC UV–Vis spectrophotometer (Shanghai Mipuda Instrument Co., Ltd., China) was adopted to quantify the absorbance of liquid part from the solid-liquid separation and the acid-soluble lignin content. Mix 0.96 ml of liquid part from the solid-liquid separation with 0.04 ml of 50 % NaOH prepared mixed solution. Waters e2695 liquid chromatography analyser was adopted to evaluate the acidified sugar concentration and calculate the composition of hemicellulose and cellulose in the liquid. The chemical functional groups of biocomposites were identified via the Nicolet IS50 Fourier transform infrared spectroscopy (Thermo Fisher Scientific) integrated with attenuation total reflection mirror in the wavelength range of 4000~400 cm^{-1}. X-ray diffraction was performed on the samples in the 2θ range of 10–50° using equipment from Beijing Puwei General Instrument Co., Ltd. located in China. The current utilised was 30 mA while the voltage chosen for operation was 40 kV.

To analyse the relative amounts of O and C atoms and binding states in the sample, the Axis Ultradld X-ray photoelectron spectroscopy device, which was assembled by Shimadzu Enterprise Management Co. Ltd. In China, was employed. The equipment was run in a vacuum environment at 7 × 10^{-8} Pa, with a current of 10 mA and AC voltage of 15 kV. The C1, C2, and C3 atomic characteristic peaks of each sample were re-adjusted for accurate measurements. The BSD-PS4 Specific Surface & Pore Size Analyzer was used for Brunauer-Emmett-Teller analysis, the degassing time was 2880 min, and the degassing temperature was 110 °C.

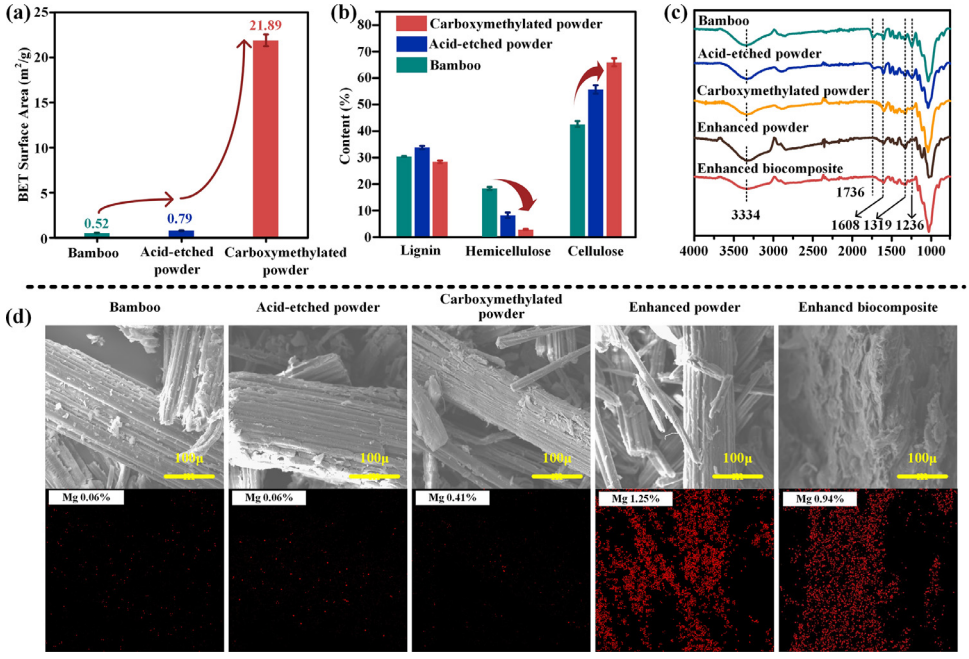

Fig. 2

(a) Specific surface area diagram of the sample; (b) The chemical composition content of each sample; (c) Infrared spectra of each sample before and after treatment. (d) EDS of these samples shows the changes in the element content of each sample.

Results and discussion

Effect of acid-etching and carboxymethylation on chemical functional groups, specific surface area, and microstructure

Fig. 2a illustrates the changes in specific surface area of the bamboo powder throughout the acid-etching and carboxymethylation stages, from 0.52 m^2/g of bamboo to 0.79 m^2/g of acid-etched powder, to 21.89 m^2/g of carboxymethylated powder. Acid treatment of the bamboo powder leads to a slight increase in specific surface area, indicating a deconstruction of the bamboo cell wall. This is attributed to the combined effects of acid treatment and ball milling [40]. The resulting breakdown of fiber bonds and removal of the branched hemicellulose causes the treated fiber to become looser and rougher (Fig. 3b), leading to a higher specific surface area [41]. The roughened surface produced by acid etching pretreatment enhances the contact area for chemical reagents, further facilitating the breakdown of hemicellulose connections. Subsequently, the hydroxyl groups are replaced by carboxymethyl groups during the carboxymethylation step, increasing potential bonding sites on the surface of the fiber; this aligns with the changes in the chemical composition (Fig. 2b). After etching, the hemicellulose content decreased sharply and the subsequent carboxymethylation treatment further amplifies this process. Moreover, the simultaneous increase in cellulose as the treatment progressed was interpreted as a decrease in the absolute content of hemicellulose resulting in an increase in the relative content of cellulose.

The results from infrared spectra indicates noticeable alterations in the functional groups of bamboo powder before and after treatment (Fig. 2c). The peak intensity detected from acid-etched powder at 1735 cm^{-1} and 1236 cm^{-1}, correspond to the carbonyl group and C–O bond, respectively. These peaks are significantly curtailed in comparison to bamboo powder, which signifies the elimination of bamboo hemicellulose. Upon carboxymethylation, the characteristic peaks at 1736 cm^{-1} and 1236 cm^{-1} vanish, suggesting the complete removal of hemicellulose. However, the peak intensity at 1608 cm^{-1} elevate while that of the peak at 3334 cm^{-1} weaken, indicating the replacement of cellulose surface hydroxyl groups with carboxyl groups (carboxymethylation). The treated bamboo powder display two distinct characteristic peaks at 2840 cm^{-1} and 1319 cm^{-1}, indicating the incorporation of Mg^{2+} [42]. It has been found that no chemical change occurs during hot pressing.

EDS analysis reveals an explicit incorporation of Mg^{2+} (Fig. 2a), where the content of Mg increases by 1.25 % after being immersed in the $MgCl_2$ solution. The decrease in Mg after hot pressing can be explained as Mg^{2+} facilitates fiber bonding by creating ionic "bridges" between fibers. On the other hand, compared to untreated bamboo powder, acid-etched bamboo powder has a lower carbon-to-oxygen ratio (Fig. S1), because the content of hemicellulose, which has more carbon-containing branched chains, is decreased during acid etching. Through carboxymethylation, the number of C=O groups increases, and the carbon-to-oxygen ratio further decreases [43], which can be evidenced in the XPS results (Fig. S2). The enhanced biocomposite exhibits a decrease in the number of C–O bonds and an increase in C=O bonds, based on changes in XPS peak areas, validating the effective elimination of hemicellulose and carboxymethylation. The change in carbon-oxygen after hot pressing can be explained by lignin precipitation on the fiber surface during hot pressing.

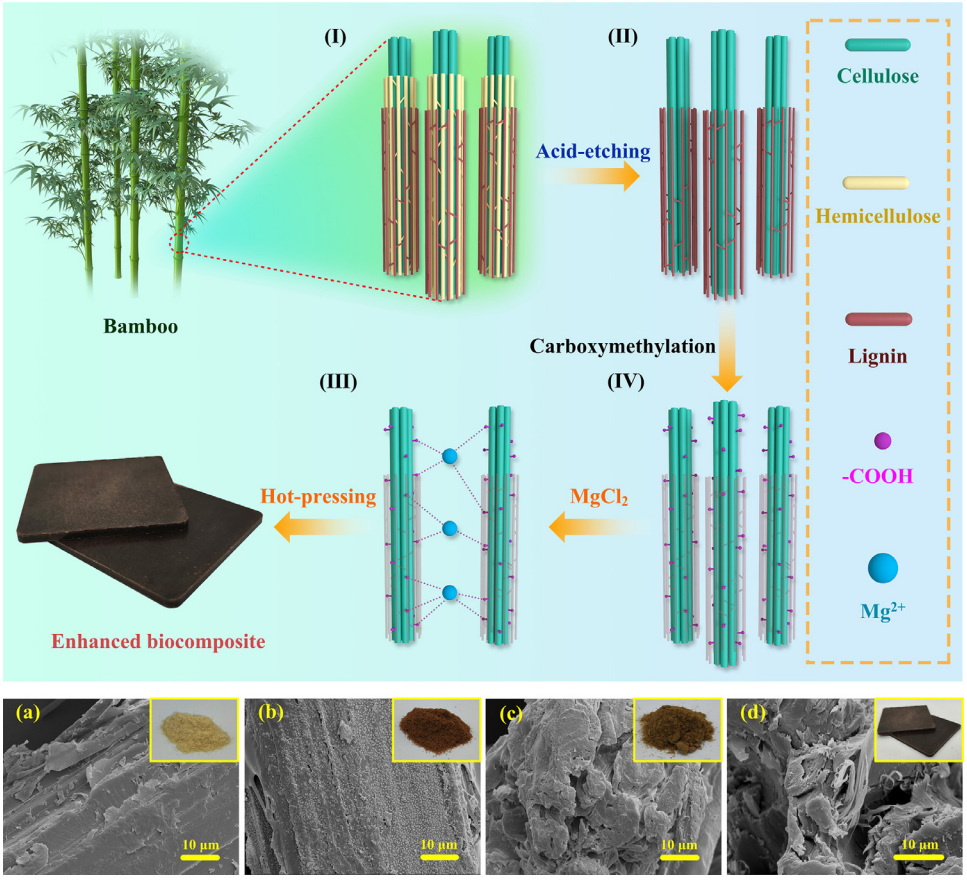

Fig. 3

Enhanced biocomposite deconstructed and reassembled schematic diagram. Bamboo cell deconstruction and fiber bonding promoted by Mg^{2+}. Microstructure of each sample (a) bamboo (b) acid-etched powder; (c) enhanced powder; (d) enhanced biocompostite.

This is prompted by the greater carbon-to-oxygen ratio of lignin compared to cellulose where it causes the overall C:O ratio to increase when precipitates onto the fiber surface.

The acid etching has a substantial impact on the surface of bamboo powder. The surface is found to become rough after treatment due to the removal of hemicellulose (Fig. 3a-d). Subsequent carboxymethylation and coordination of Mg^{2+} led to further shrinking of material surface, resulting in the re-agglomeration of fibers and yellow colouration of the powder (Fig. 3c). At last, hot pressing caused the repolymerization of fibers, which recombine them into a single fiber (Fig. 3d).

Mechanical properties of enhanced bamboo biocomposites

In Fig. 4a and b, a significant enhancement in the mechanical properties of biocomposite is observed. The flexural strength is recorded at 104.14 MPa, with the tensile strength captured at 94.24 MPa. In comparison, the control biocomposite exhibits lower strength of 27.87 MPa and 14.38 MPa for flexural and tensile strengths, respectively. Also, the stretchability increased from 14 MPa to 94.24 MPa due to improved mechanical properties brought by the coordination between Mg^{2+} ions and the carboxyl groups. It is important that the concentration of the $MgCl_2$ solution used is high enough (30 wt.%), to ensure that sufficient coordination bonds are formed between Mg^{2+} ions and fibers. Insufficient $MgCl_2$ concentrations could lead to suboptimal Mg^{2+} coordination, resulting in low mechanical strength (Fig. S2).

The mechanical properties of the enhanced biocomposite are further improved through a simple acid-etching pretreatment. This is reflected in the improvement of mechanical properties of acid-etched biocomposites. This pretreatment effectively removes hemicellulose from the material, allows lignin to occupy the spaces between fibers during hot pressing [44]. This increase in mechanical strength is attributed to the denser structure provided by hot pressing. However, it is imperative to note that the connection between fibers and lignin still depends on hydrogen bonding provided by high temperatures and high pressure. As a result, improvement in mechanical strength is limited in the control samples that have no Mg^{2+} ions. The introduction of Mg^{2+} addresses this constraint by reinforcing the connection between the fibers and lignin. This approach forms coordination bonds that are stronger and more robust than hydrogen bonds, leading to denser and structurally more stable materials [45]. The introduction of Mg^{2+} made this new type of binding possible. As a result, the enhanced biocomposite exhibits a substantially higher elastic modulus, with a bending modulus of 21.29 GPa and a tensile modulus of 7.01 GPa, compared to both the acid-etching biocomposite (12.71 GPa, 4.72 GPa) and the control biocomposite

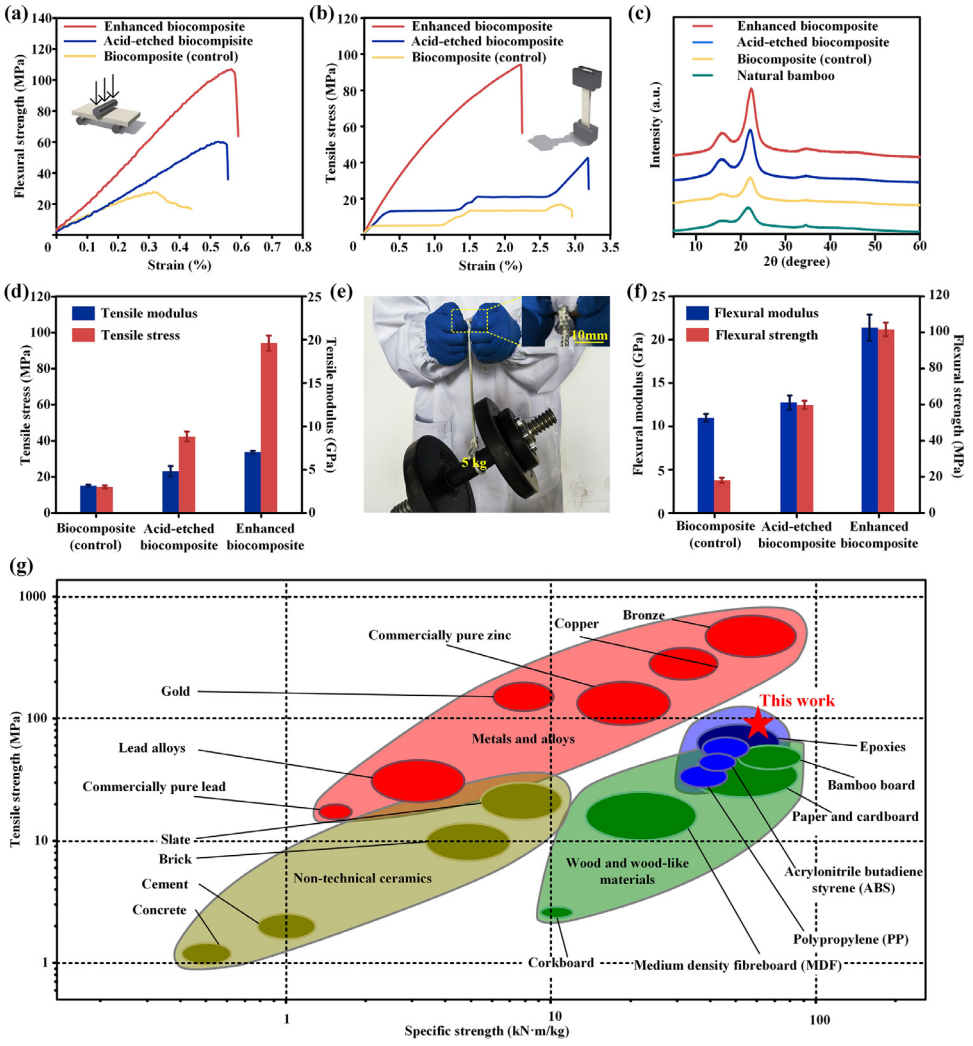

Fig. 4

(a) flexural stress-strain diagram of the sample; (b) tensile stress-strain diagram of the sample; (c) XRD of the sample; (d) tensile strength and modulus; (e) a demonstration of the mechanical properties of enhanced biocomposite; (f) flexural strength and modulus; (g) an Ashby Chart comparing the specific strength and tensile strength with common materials.

(12.71 GPa, 3.19 GPa). This enhanced combination of elements significantly increases the rigidity of the material (Fig. 4d-4f).

The modification in the crystalline structure of material is evidenced from the X-ray diffraction (XRD), which consequently accounts for the enhancement in the mechanical strength, as shown in Fig. 4c. The calculation for determining the crystallinity is represented by the equation below:

$$CrI = \left(1 - \frac{I_{am}}{I_{002}}\right) \times 100\%$$

The data presented in Table 1 reveal that the enhanced bamboo biocomposite exhibits a higher cellulose crystallinity level of 62.32 %, in contrast to the 50.24 % found in natural bamboo. This increase in crystallisation area can be attributed to the presence of Mg^{2+} in the material, which promotes a more compact fiber combination. Furthermore, the acid etching treatment applied to the bamboo material breaks down its cell wall and hemicellulose, thereby exposing it to chemical reagents that enhance subsequent processing and further enhance crystallinity [46–47]. In addition to its enhanced crystallinity, the reinforced bamboo biocomposite also demonstrates robust mechanical properties (Fig. 4e), this allows some less demanding engineering materials to be replaced by it. The glue-free strategy also allows for completely recycling raw materials from waste bamboo or even the reinforced biocomposite itself. As a result of its increased crystallinity and robust mechanical properties,

Table 1

Crystallinity of each sample.

Sample	Crystallinity (%)
Bamboo	50.24
Biocomposite (control)	52.69
Acid-etched biocomposite	53.5
Enhance bamboo biocomposite	62.32

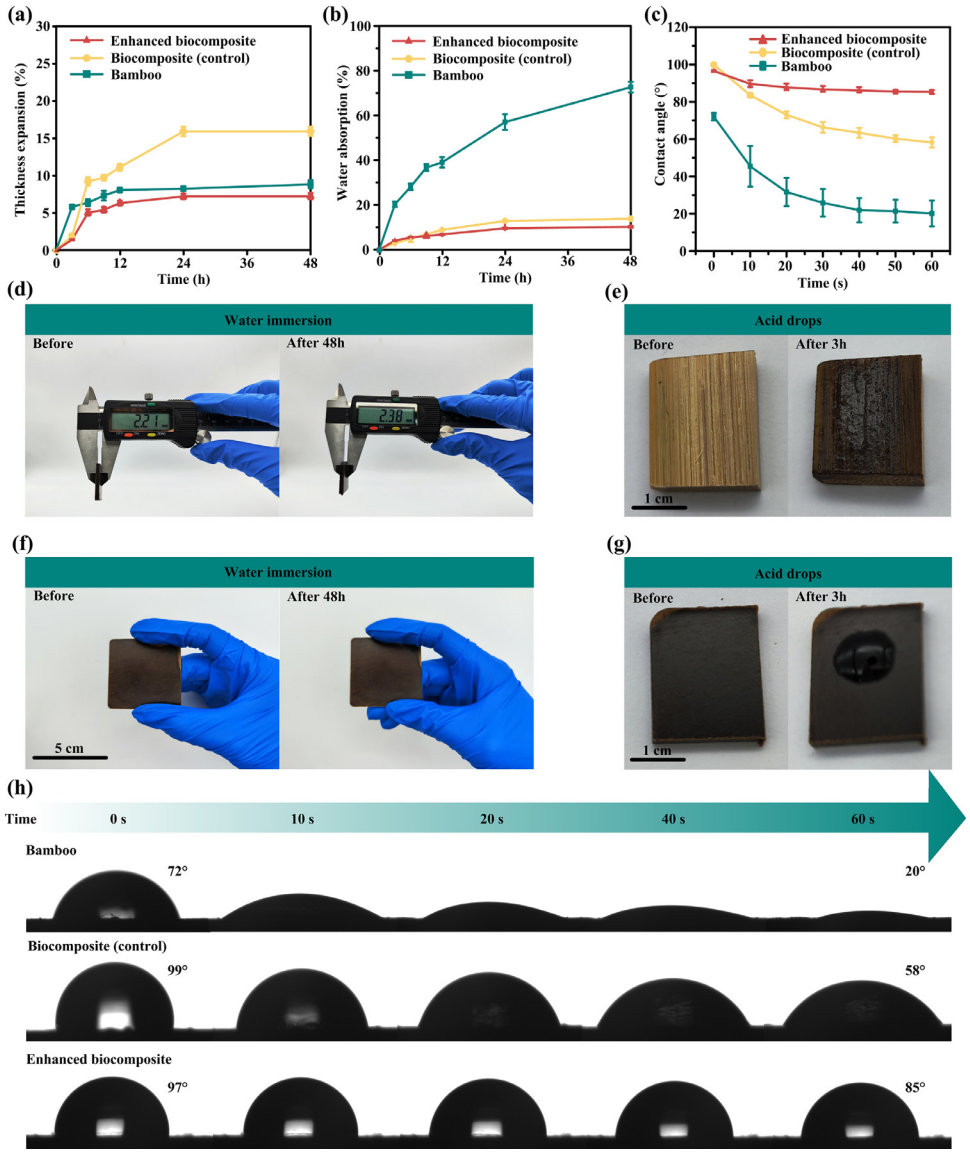

Fig. 5

(a) 48 h water absorption thickness expansion of the materials; (b) 48 h water absorption of the materials; (c) change of contact angle of each sample within 60 s; (d) enhanced biocomposite thickness changes before and after 48 h in the water environment; (e) The bamboo was dripping with acid; (f) change of macromorphology of enhanced biocomposite in the water environment; (g) The enhanced biocomposite was dripping with acid; (h) Sample contact angle picture.

the reinforced bamboo biocomposite has the possibility to be employed in several engineering purposes as showcased in Fig. 4g.

The water resistance of enhanced bamboo biocomposites

It is found that the water absorption and thickness expansion of enhanced biocomposite is significantly lower than the biocomposite (control) and natural bamboo samples (Fig. 5a). The low thickness expansion can make the material obtain a more stable form in outdoor environment or high humidity conditions. Specifically, the water absorption thickness expansion percentage of enhanced biocomposite is only 7.21 %. After 48 h, the biocomposite (control) and natural bamboo samples exhibit 15.9 % and 8.9 % expansion, respectively. Additionally, the enhanced biocomposite material retains its appearance and structure even after being immersed in water for another 48 h (Fig. 5d, f), which is not the case for the control sample, where hydrogen bonds are easily broken down in this kind of environment. The water resistance of the enhanced biocomposite is facilitated by the coordination of magnesium ions, which prevents the fibers from disintegrating in water [48–49]. This is manifested by a decrease in the number of free hydroxyl groups, which is due to the substitution of hydroxyl groups in pretreatment and the further increase in crystallinity after hot pressing.

The rate of weight gain in samples provides a vital measure for assessing the water resistance of the material. Due to the porous structure and cellular cavities, bamboo exhibits a higher water absorption rate compared to the other two samples (Fig. 5b). Conversely, the enhanced biocomposite sample undergoes densification and surface hydroxyl group destruction

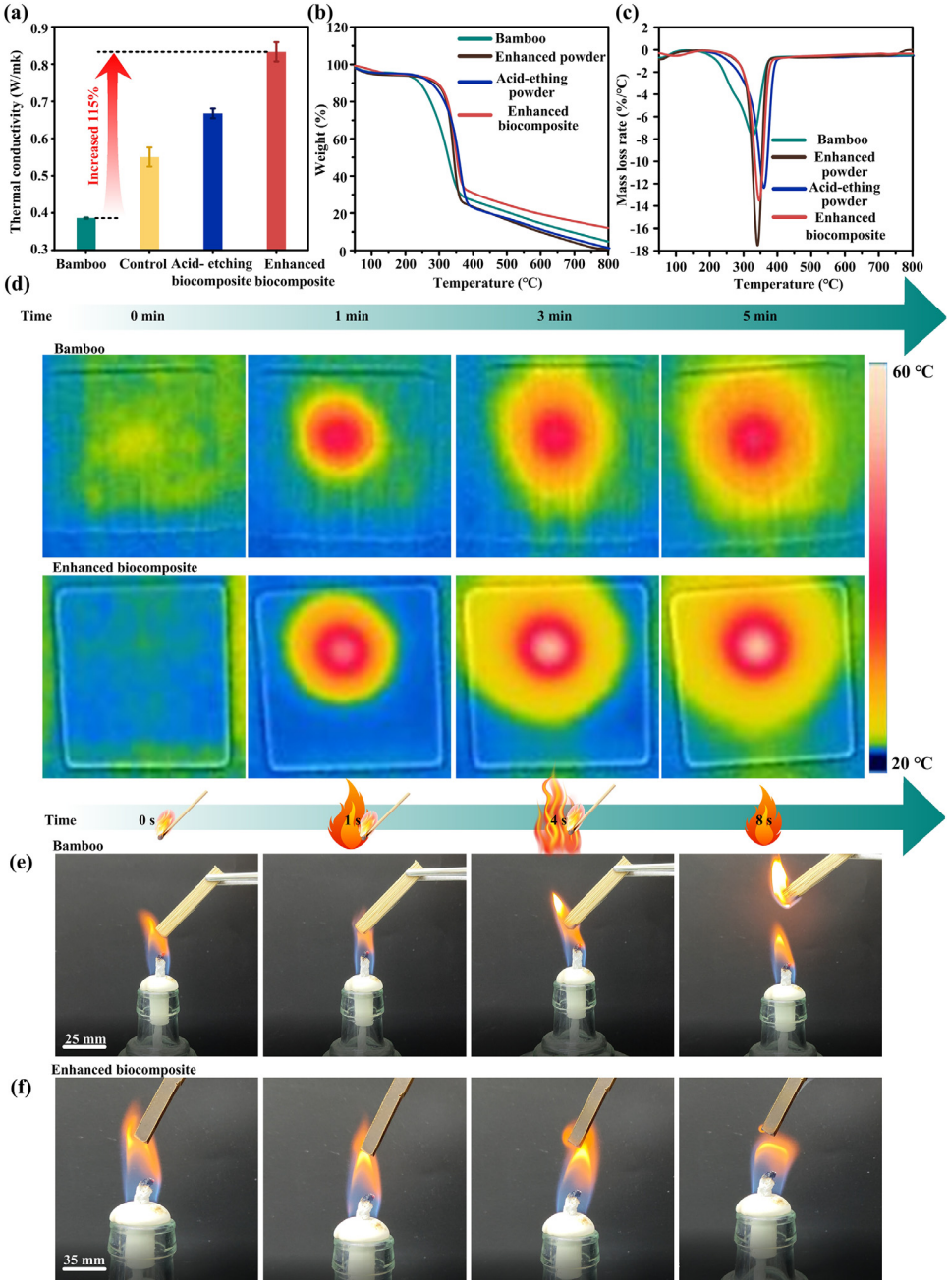

Fig. 6

(a) Thermal conductivity of a material; (b) Variation diagram of the residual mass of material with temperature (TG of the materials); (c) Variation diagram of the mass change rate of material with temperature (DTG of the materials); (d) Thermal image of each sample. Combustion of bamboo, enhanced biocomposite under the flame of an alcohol lamp.

during hot pressing, resulting in a significantly lower water content of only 10.27 % after 48 h. The hot-pressing process also results in a high contact angle for the material due to lignin deposition on its surface. Despite this, the advancements in fiber bonding techniques have resulted in an improved biocomposite that maintains a contact angle of 85.3° for 60 s (Fig. 5c, h), indicating a hydrophobic nature. Upon exposure to concentrated sulfuric acid droplets (72 wt%) for 3 h, the bamboo surface undergoes complete blackening owing to the infiltration of the acid solution and the oxidation of the fiber surface. In contrast, the reinforced biocomposite remains unscathed, with droplets resting on its surface thereby maintaining its structural integrity even under acidic conditions (Fig. 5e, g).

Thermal conductivity and flame retardancy of enhanced bamboo biocomposites

The enhanced bio-composites possess the highest thermal conductivity (Fig .6a). Fig. 6b presents the percentage mass change of the material as temperature increases. Remarkably, surface activation and embedding of Mg^{2+} significantly improve the heat

resistance. The degradation temperature range of hemicellulose is between 225 and 300 °C, during which bamboo quality decreases rapidly. However, the rest samples remain unchanged, suggesting the efficient removal of hemicellulose. The degradation of hemicellulose is observed between 270 and 370 °C. The quality of acid-etch powder rapidly declines between 275 and 325 °C due to the hemicellulose residue and fiber combination. Destroyed cell walls more likely lead to the degradation.

Between 325–375 °C, the enhanced powder degrade rapidly and reach its maximum degradation rate at around 350 °C, which is slightly lower than that of the acid-etched powder sample (Fig. 6c) [50–51]. This phenomenon is caused by the replacement of functional groups on the fiber surface. Acid-etched treatment replaces hydroxyl groups with carboxyl groups, reducing cellulose thermal degradation temperature. After hot pressing, making the materials more closely bonded, thus improving thermal stability. The enhanced biocomposite has a lower maximum degradation rate than the enhanced powder without hot pressing (Fig. 6c), and a higher temperature was required to reach the maximum degradation rate. This is due to the increased bonding after hot pressing. A laser with a power of 0.5 W and a wavelength of 808 nm were used to irradiate the surface of the sheet with a spot diameter of 10 mm. The infrared thermal imager shows the temperature rise after being irradiated by light. The enhanced biocomposite has higher thermal conductivity, making it easier to disperse the heat to other areas, thus reducing the heating time (Fig. 6d).

The flame retardancy is a critical application requirement for bamboo-based bio-composite. Due to the porous structure and loose build, it is highly susceptible to combustion with rapid spreading [52–53]. When exposed to an alcohol lamp flame, ignition occurs within 4 s and spreads to all parts of the front end with the potential for self-ignition within 8 s (Fig. 6e). However, the dense structure and surface deposition of lignin resulting from hot pressing has significantly improved the flame-retardant of material. The biocomposite (control) burns weakly at 4 s and only a tiny flame remains at the end when it leaves the flame for 8 s (Fig. S4).The enhanced flame retardancy of the material can be attributed to the further dense structure and Mg^{2+} addition [54]. Upon ignition, the enhanced biocomposite burns with only tiny flames gathering at the end in 4 s and burns out quickly when it leaves the alcohol lamp flame in 8 s, thus demonstrating its flame-retardant ability (Fig. 6f). It is notable from the aforementioned findings that the flame retardancy of the material is drastically enhanced through the addition of magnesium and the resulting dense structure.

Conclusion

In this work, we describe a novel facile fabrication of a glue-free bamboo biocomposite for fiberboard. Our methods involve a pretreatment process where bamboo powder is etched using acetic acid and ball milling, effectively deconstructing the bamboo cell wall. This is followed by the incorporation of carboxymethyl into the bamboo fiber, which significantly improves its surface activity and provides reaction sites for Mg^{2+}ions. This synergy between Mg^{2+} ions and carboxyl groups (COO^{-}) facilitates fiber bonding allowing for the formation of a denser structure during hot pressing. The obtained enhanced biocomposite material has high tensile strength (94.24 MPa) and flexural strength (104.14 MPa), which are significantly improved compared to the tensile strength (14 MPa) and flexural strength (27.87 MPa) of glue-free bamboo fiber board. Under 12 h of water soaking, the enhanced biocomposite (6.8 %) was far stronger than the glue-free bamboo fiber board (9 %). The thermal conductivity and fire retardancy have been explored with improved performance. Based on this strategy, numerous application scenarios have been expanded including construction, outdoor decoration, and other areas previously unavailable due to fiberboard defects. Moreover, the fabrication process is devoid of harmful emissions and the resources are reusable. We expect this glue-free bamboo fiber board technique to find wider application venue as a sustainable and green material in the construction industry.

Funding

The authors thank the National Natural Science Foundation of China (32201491), China Postdoctoral Science Foundation (2021M690847), Young Elite Scientists Sponsorship Program by CAST (2023QNRC001). BBX is grateful for the support from the Engineering and Physical Sciences Research Council (EPSRC, UK) grants - EP/N007921.

Declaration of competing interest

The authors declare that they have no known competing financial interests or personal relationships that could have appeared to influence the work reported in this paper.

Data availability

Supporting Information is available from the Wiley Online Library or from the author.

CRediT authorship contribution statement

Shengbo Ge: Writing – review & editing, Writing – original draft, Visualization, Validation, Supervision, Software, Resources, Project administration, Methodology, Investigation, Funding acquisition, Formal analysis, Data curation, Conceptualization. **Guiyang Zheng:** Project administration, Methodology, Investigation, Formal analysis, Data curation, Conceptualization. **Yang Shi:** Writing – original draft, Visualization, Validation, Software, Methodology, Investigation. **Zhongfeng Zhang:** Visualization, Validation, Supervision, Resources, Project administration, Methodology, Investigation, Formal analysis, Data curation. **Abdullatif Jazzar:** Writing – original draft, Validation, Software, Methodology, Investigation, Formal analysis. **Ximin He:** Writing – review & editing, Writing – original draft, Visualization, Validation, Supervision, Software, Methodology. **Saddick Donkor:** Writing – original draft, Visualization, Validation, Methodology, Formal analysis. **Zhanhu Guo:** Validation, Supervision, Software, Resources, Methodology, Investigation, Formal analysis, Data curation, Conceptualization. **Ding Wang:** Visualization, Validation, Methodology, Formal analysis, Data curation, Conceptualization.

Acknowledgements

The funding has been acknowledged in the following section.

Supplementary materials

Supplementary material associated with this article can be found, in the online version, at doi:10.1016/j.giant.2024.100253.

References

[1] A. Di Sacco, K.A. Hardwick, D. Blakesley, P.H. Brancalion, E. Breman, L. Cecilio Rebola, S. Chomba, K. Dixon, S. Elliott, G. Ruyonga, Ten golden rules for reforestation to optimize carbon sequestration, biodiversity recovery and livelihood benefits, Glob. Chang. Biol. 27 (2021) 1328–1348.

[2] A. Benítez, J. Amaro-Gahete, Y.C. Chien, Á. Caballero, J. Morales, D. Brandell, Recent advances in lithium-sulfur batteries using biomass-derived carbons as sulfur host, Renew. Sust. Energ. Rev. 154 (2022) 111783.

[3] M. Sajjadi, F. Ahmadpoor, M. Nasrollahzadeh, H. Ghafuri, Lignin-derived (nano) materials for environmental pollution remediation: current challenges and future perspectives, Int. J. Biol. Macromol. 178 (2021) 394–423.

[4] R. Qin, G. Shan, M. Hu, W. Huang, Two-dimensional transition metal carbides and/or nitrides (MXenes) and their applications in sensors, Mater. Today Phys. 21 (2021) 100527.

[5] A. Quisperima, S. Pérez, E. Flórez, N. Acelas, Valorization of potato peels and eggshells wastes: ca-biocomposite to remove and recover phosphorus from domestic wastewater, Bioresour. Technol. 343 (2022) 126106.

[6] C.M. Costa, J.C. Barbosa, R. Gonçalves, H. Castro, F. Del Campo, S. Lanceros-Méndez, Recycling and environmental issues of lithium-ion batteries: advances, challenges and opportunities, Energy Stor. Mater. 37 (2021) 433–465.

[7] J.M. Millican, S. Agarwal, Plastic pollution: a material problem? Macromolecules 54 (2021) 4455–4469.

[8] O.A. Oyewo, E.E. Elemike, D.C. Onwudiwe, M.S. Onyango, Metal oxide-cellulose nanocomposites for the removal of toxic metals and dyes from wastewater, Int. J. Biol. Macromol. 164 (2020) 2477–2496.

[9] M. Shen, W. Huang, M. Chen, B. Song, G. Zeng, Y. Zhang, Micro) plastic crisis: un-ignorable contribution to global greenhouse gas emissions and climate change, J. Clean. Prod. 254 (2020) 120138.

[10] M. Shen, B. Song, G. Zeng, Y. Zhang, W. Huang, X. Wen, W. Tang, Are biodegradable plastics a promising solution to solve the global plastic pollution? Environ. Pollut 263 (2020) 114469.

[11] K.H. Vardhan, P.S. Kumar, R.C. Panda, A review on heavy metal pollution, toxicity and remedial measures: current trends and future perspectives, J. Mol. Liq. 290 (2019) 111197.

[12] D. Merino, A.I. Quilez-Molina, G. Perotto, A. Bassani, G. Spigno, A. Athanassiou, A second life for fruit and vegetable waste: a review on bioplastic films and coatings for potential food protection applications, Green Chem. (2022).

[13] M.F. Rosa, B.S. Chiou, E.S. Medeiros, D.F. Wood, T.G. Williams, L.H. Mattoso, W.J. Orts, S.H. Imam, Effect of fiber treatments on tensile and thermal properties of starch/ethylene vinyl alcohol copolymers/coir biocomposites, Bioresour. Technol. 100 (2009) 5196–5202.

[14] A.P. Kumar, R.P. Singh, Biocomposites of cellulose reinforced starch: improvement of properties by photo-induced crosslinking, Bioresour. Technol. 99 (2008) 8803–8809.

[15] M. Mujtaba, L. Fraceto, M. Fazeli, S. Mukherjee, S.M. Savassa, G.A. de Medeiros, A. d. E. Santo Pereira, S.D. Mancini, J. Lipponen, F. Vilaplana, Lignocellulosic biomass from agricultural waste to the circular economy: a review with focus on biofuels, biocomposites and bioplastics, J. Clean. Prod (2023) 136815.

[16] W. Sun, M. Tajvidi, C.G. Hunt, B.J. Cole, C. Howel, D.J. Gardner, J. Wang, Fungal and enzymatic pretreatments in hot-pressed lignocellulosic bio-composites: a critical review, J. Clean. Prod. (2022) 131659.

[17] H. Wang, X. Li, X. Zhao, C. Li, X. Song, P. Zhang, P. Huo, A review on heterogeneous photocatalysis for environmental remediation: from semiconductors to modification strategies, Chinese J. Catal. 43 (2022) 178–214.

[18] W. Cai, Z. Luo, J. Zhou, Q. Wang, A review on the selection of raw materials and reactors for biomass fast pyrolysis in China, Fuel Process. Technol. 221 (2021) 106919.

[19] Y. Ai, L. Zhang, M. Cui, R. Huang, W. Qi, Z. He, J.J. Klemeš, R. Su, Toward cleaner production of nanocellulose: a review and evaluation, Green Chem (2022).

[20] P. Xu, J. Zhu, H. Li, Z. Xiong, X. Xu, Coupling analysis between cost and carbon emission of bamboo building materials: a perspective of supply chain, Energy Build. 280 (2023) 112718.

[21] L. Chen, K. Zhang, J. Ahn, F. Wang, Y. Sun, J. Lee, J.Y. Cheong, C. Ma, H. Zhao, G. Duan, Morph-genetic bamboo-reinforced hydrogel complex for bio-mimetic actuator, Chem. Eng. J. 463 (2023) 142391.

[22] C. Huang, Y. Zhan, J. Cheng, J. Wang, X. Meng, G. Fang, A.J. Ragauskas, The bamboo delignification saturation point in alkaline hydrogen peroxide pretreatment and its association with enzymatic hydrolysis, Bioresour. Technol. 359 (2022) 127462.

[23] T. Yuan, X. Wang, Z. Lou, T. Zhang, X. Han, Z. Wang, X. Hao, Y. Li, Comparison of the fabrication process and macro and micro properties of two types of crack-free, flatten bamboo board, Constr. Build. Mater. 317 (2022) 125949.

[24] J. Deng, X. Wei, H. Zhou, G. Wang, S. Zhang, Inspiration from table tennis racket: preparation of rubber-wood-bamboo laminated composite (RWBLC) and its response characteristics to cyclic perpendicular compressive load, Compos. Struct. 241 (2020) 112135.

[25] J. Wang, X. Wu, Y. Wang, W. Zhao, Y. Zhao, M. Zhou, Y. Wu, G. Ji, Green, Sustainable architectural bamboo with high light transmission and excellent electromagnetic shielding as a candidate for energy-saving buildings, Nanomicro Lett. 15 (2023) 11.

[26] S. Ge, N.L. Ma, S. Jiang, Y.S. Ok, S.S. Lam, C. Li, S.Q. Shi, X. Nie, Y. Qiu, D. Li, Processed bamboo as a novel formaldehyde-free high-performance furniture biocomposite, ACS Appl. Mater. Interfaces 12 (2020) 30824–30832.

[27] C. Xu, G. Dai, Y. Hong, Recent advances in high-strength and elastic hydrogels for 3D printing in biomedical applications, Acta Biomater. 95 (2019) 50–59.

[28] H. Tu, M. Zhu, B. Duan, L. Zhang, Recent progress in high-strength and robust regenerated cellulose materials, Adv. Mater. 33 (2021) 2000682.

[29] F. Zou, A. Manthiram, A review of the design of advanced binders for high-performance batteries, Adv. Eng. Mater. 10 (2020) 2002508.

[30] P. Wang, Y. Wu, B. Cai, Q. Ma, X. Zheng, W.H. Zhang, Solution-processable perovskite solar cells toward commercialization: progress and challenges, Adv. Funct. Mater. 29 (2019) 1807661.

[31] M. Li, Y. Pu, V.M. Thomas, C.G. Yoo, S. Ozcan, Y. Deng, K. Nelson, A.J. Ragauskas, Recent advancements of plant-based natural fiber–reinforced composites and their applications, Compos. B. Eng. 200 (2020) 108254.

[32] S. Fadlallah, P.S. Roy, G. Garnier, K. Saito, F. Allais, Are lignin-derived monomers and polymers truly sustainable? An in-depth green metrics calculations approach, Green. Chem. 23 (2021) 1495–1535.

[33] G. Zheng, H. Ye, Y. Liang, X. Jin, C. Xia, W. Fan, Y. Shi, Y. Xie, J. Li, S. Ge, Pre-treatment of natural bamboo for use as a high-performance bio-composites via acetic acid ball milling technology, Constr. Build. Mater. 367 (2023) 130350.

[34] D. Jubinville, E. Esmizadeh, C. Tzoganakis, T. Mekonnen, Thermo-mechanical recycling of polypropylene for the facile and scalable fabrication of highly loaded wood plastic composites, Compos. B. Eng. 219 (2021) 108873.

[35] S. Yang, B. Wei, Q. Wang, Superior dispersion led excellent performance of wood-plastic composites via solid-state shear milling process, Compos. B Eng. 200 (2020) 108347.

[36] S. Gao, E. Mäder, R. Plonka, Nanostructured coatings of glass fibers: improvement of alkali resistance and mechanical properties, Acta Mater. 55 (2007) 1043–1052.

[37] Q. Li, A. Omar, W. Cha-Umpong, Q. Liu, X. Li, J. Wen, Y. Wang, A. Razmjou, J. Guan, R.A. Taylor, The potential of hollow fiber vacuum multi-effect membrane distillation for brine treatment, *Appl. Energy* 276 (2020) 115437.

[38] F. Chen, Z. Jiang, G. Wang, H. Li, L.M. Simth, S.Q. Shi, The bending properties of bamboo bundle laminated veneer lumber (BLVL) double beams, Constr. Build Mater. 119 (2016) 145–151.

[39] Y. Liang, G. Zheng, C. Xia, S. Zuo, S. Ge, R. Yang, X. Ma, B. Fei, J. Li, C.K. Cheng, Synthesis of ultra-high strength structured material from steam-modified delignification of wood, J. Clean. Prod. 351 (2022) 131531.

[40] D. Xin, Z. Yang, F. Liu, X. Xu, J. Zhang, Comparison of aqueous ammonia and dilute acid pretreatment of bamboo fractions: structure properties and enzymatic hydrolysis, Bioresour. Technol. 175 (2015) 529–536.

[41] X. Guo, Y. Wang, Y. Ren, X. Liu, Fabrication of flame retardant lyocell fibers based on carboxymethylation and aluminum ion chelation, Cellulose 28 (2021) 6679–6698.

[42] Y.Y. Wang, X.Q. Wang, Y.Q. Li, P. Huang, B. Yang, N. Hu, S.Y. Fu, High-performance bamboo steel derived from natural bamboo, ACS Appl. Mater. Interfaces 13 (2020) 1431–1440.

[43] W. Yang, B. Tawiah, C. Yu, Y.F. Qian, L.L. Wang, A.C.Y. Yuen, S.E. Zhu, E.Z. Hu, T.B.Y. Chen, B. Yu, Manufacturing, mechanical and flame retardant properties of poly (lactic acid) biocomposites based on calcium magnesium phytate and carbon nanotubes, Compos. Part A Appl. Sci. Manuf. 110 (2018) 227–236.

[44] K. Jin, L. Kong, X. Liu, Z. Jiang, G. Tian, S. Yang, L. Feng, J. Ma, Understanding the xylan content for enhanced enzymatic hydrolysis of individual bamboo fiber and parenchyma cells, ACS. Sustain. Chem. Eng. 7 (2019) 18603–18611.

[45] Q.F. Guan, Z.M. Han, H.B. Yang, Z.C. Ling, S.H. Yu, Regenerated isotropic wood, Natl. Sci. Rev. 8 (2021) nwaa230.

[46] T. Yuan, X. Xiao, T. Zhang, Z. Yuan, X. Wang, Y. Li, Preparation of crack-free, non-notched, flattened bamboo board and its physical and mechanical properties, Ind. Crops. Prod. 174 (2021) 114218.

[47] T. Yuan, X. Wang, X. Liu, Z. Lou, S. Mao, Y. Li, Bamboo flattening technology ebables efficient and value-added utilization of bamboo in the manufacture of furniture and engineered composites, Compos. B: Eng. 242 (2022) 110097.

[48] X. Ji, B. Li, B. Yuan, M. Guo, Preparation and characterizations of a chitosan-based medium-density fiberboard adhesive with high bonding strength and water resistance, Carbohydr. Polym. 176 (2017) 273–280.

[49] C. Liu, B. Yuan, M. Guo, Q. Yang, T.T. Nguyen, X. Ji, Effect of sodium lignosulfonate on bonding strength and chemical structure of a lignosulfonate/chitosan-glutaraldehyde medium-density fiberboard adhesive, Adv. Compos. Hybrid Ma 4 (2021) 1176–1184.

[50] Q. Liu, S. Wang, Y. Zheng, Z. Luo, K. Cen, Mechanism study of wood lignin pyrolysis by using TG–FTIR analysis, J. Anal. Appl. Pyrolysis 82 (2008) 170–177.

[51] Z.Z. Li, Y. Luan, J.B. Hu, C.H. Fang, L.T. Liu, Y.F. Ma, Y. Liu, B.H. Fei, Bamboo heat treatments and their effects on bamboo properties, Constr. Build. Mater. 331 (2022) 127320.

[52] J. Mena, S. Vera, J.F. Correal, M. Lopez, Assessment of fire reaction and fire resistance of Guadua angustifolia kunth bamboo, Constr. Build. Mater. 27 (2012) 60–65.

[53] J. Yu, D. Yang, Q. He, B. Du, S. Zhang, M. Hu, Strong, durable and fire-resistant glass fiber-reinforced bamboo scrimber, Ind. Crops. Prod. 181 (2022) 114783.

[54] M. Dogan, S.D. Dogan, L.A. Savas, G. Ozcelik, U. Tayfun, Flame retardant effect of boron compounds in polymeric materials, Compos. B. Eng. 222 (2021) 109088.